Article

Surface Casimir Densities on Branes Orthogonal to the Boundary of Anti-De Sitter Spacetime

Aram Saharian [ID]

Institute of Physics, Yerevan State University, 1 Alex Manogian Street, Yerevan 0025, Armenia; saharian@ysu.am

Abstract: The paper investigates the vacuum expectation value of the surface energy–momentum tensor (SEMT) for a scalar field with general curvature coupling in the geometry of two branes orthogonal to the boundary of anti-de Sitter (AdS) spacetime. For Robin boundary conditions on the branes, the SEMT is decomposed into the contributions corresponding to the self-energies of the branes and the parts induced by the presence of the second brane. The renormalization is required for the first parts only, and for the corresponding regularization the generalized zeta function method is employed. The induced SEMT is finite and is free from renormalization ambiguities. For an observer living on the brane, the corresponding equation of state is of the cosmological constant type. Depending on the boundary conditions and on the separation between the branes, the surface energy densities can be either positive or negative. The energy density induced on the brane vanishes in special cases of Dirichlet and Neumann boundary conditions on that brane. The effect of gravity on the induced SEMT is essential at separations between the branes of the order or larger than the curvature radius for AdS spacetime. In the considerably large separation limit, the decay of the SEMT, as a function of the proper separation, follows a power law for both massless and massive fields. For parallel plates in Minkowski bulk and for massive fields the fall-off of the corresponding expectation value is exponential.

Keywords: Casimir effect; anti-de Sitter space; surface energy; Robin boundary conditions

1. Introduction

Among the interesting directions in the development of the Casimir effect theory (for a general introduction and applications, see, e.g., [1–6]) is the study of the dependence of expectation values of physical characteristics for quantum fields on the bulk and boundary geometries, as well as on the spatial topology. The interest is motivated by applications in gravitational physics, in cosmology, and in condensed matter physics. Exact analytic expressions for physical characteristics are obtained in geometries with a sufficient degree of symmetry. In particular, the corresponding background geometries include maximally symmetric spacetimes sourced by positive and negative cosmological constants. These geometries, referred as de Sitter (dS) and anti-de Sitter (AdS) spacetimes, respectively, are among the most popular bulks in quantum field theory on curved backgrounds.

The goal of this paper is to investigate the surface Casimir densities on two parallel branes for a scalar field in AdS spacetime. Quantum field theoretical effects on a fixed AdS background have been extensively studied in the literature. These investigations are important for several reasons. The AdS spacetime is a non-globally hyperbolic manifold with a timelike boundary at spatial infinity and the early interest in the formulation of quantum field theory in that geometry was related to principal questions of quantization [7–9] (see also the references in Ref. [10]). The necessity to control the information through the spatial infinity requires the imposition of boundary conditions on quantum fields (for a discussion of possible boundary conditions on the AdS boundary, see, e.g., [11,12]). The different boundary conditions correspond to physically different field theories. The AdS boundary at spatial infinity plays a central role in models of AdS/conformal field

theory (AdS/CFT) correspondence [13–16]. The latter establishes duality between conformal field theory living on the boundary of AdS spacetime and supergravity or string theory on AdS bulk. This holographic correspondence between two different theories provides an efficient computational framework for non-perturbative effects, mapping them to the perturbative region of the dual theory. Within this approach interesting results have been obtained in high energy physics, in quantum chromodynamics, and in condensed matter physics [14,17,18]. The braneworld models [19] with large extra dimensions, both phenomenological- and string-theory-motivated, present another interesting setup where the properties of AdS spacetime play a crucial role. They provide a geometrical solution to the hierarchy problem between the electroweak and gravitational energy scales and serve as an interesting framework to discuss the problems in high energy physics, gravitation, and cosmology.

The braneworld models contain two types of field: fields propagating in the bulk and fields localized on the branes. In simplified models, the interaction between branes and bulk fields is reduced to boundary conditions on the branes. Those conditions modify the spectrum of vacuum fluctuations of bulk quantum fields and give rise to the Casimir-type contributions in the expectation values of physical observables, such as the ground state energy and the vacuum forces acting on the branes. The Casimir energy and forces in the geometry of branes parallel to the AdS boundary have been widely studied in the literature (see [20–35] for early investigations and [36] for a more complete list of references). The Casimir forces can be used as a possible mechanism for stabilization of the interbrane distance that is required to escape the variations in physical constants in the effective theory on the branes. The vacuum fluctuations of the bulk field may also provide a mechanism for the generation of the cosmological constant on branes. More detailed information on the properties of the vacuum state is contained in the expectation values of bilinear combinations of fields, such as the field squared and the energy–momentum tensor. In braneworld models on AdS bulk, those expectation values are considered in Refs. [32,37–45] for scalar, fermionic, and electromagnetic fields.

In the references cited above, the branes are parallel to the AdS boundary (Randall–Sundrum-type models [46,47]). In a number of recent developments in conformal field theories, additional boundaries are present (see, e.g., [48] and references therein). In the context of AdS/CFT correspondence, the corresponding dual theory on the AdS bulk contains boundaries intersecting the AdS boundary (AdS/BCFT correspondence) [49,50]. Another interesting problem on AdS bulk with surfaces crossing its boundary is related to the evaluation of the entanglement entropy of a quantum system in conformal field theory with a boundary. In accordance with the procedure suggested in Refs. [51,52], the entanglement entropy in a bounded region from the CFT side on the AdS boundary is expressed in terms of the area of the minimal surface in the AdS bulk that asymptotes the boundary of CFT (see also [53,54] for reviews). Motivated by those developments, the influence of branes orthogonally intersecting the AdS boundary on the local properties of the scalar vacuum in a general number of spatial dimensions was studied in Refs. [55,56]. As local characteristics of the vacuum state, the expectation values of the field squared and of the energy–momentum tensor were considered. By using the corresponding vacuum stresses, the Casimir forces acting on the branes were investigated as well. It was shown that, in addition to the component perpendicular to the brane, those forces have a nonzero parallel component (shear force). In quantum field theory with boundaries, the expectation values of physical quantities may contain contributions localized on the boundary. The expression for the surface energy–momentum tensor of a scalar field with a general curvature coupling parameter, and for general bulk and boundary geometries, was derived in Ref. [57] by using the standard variational procedure. The corresponding vacuum expectation value in the problem with branes parallel to the AdS boundary was investigated in Refs. [58,59]. The present paper considers the vacuum expectation value of the surface energy–momentum tensor (SEMT) for a scalar field in the problem with two parallel branes orthogonal to the AdS boundary.

The organization of the paper is as follows. Section 2 describes the geometry of the problem and present the expression for the surface energy–momentum tensor. The corresponding vacuum expectation value (VEV) is investigated in Section 3 by using the two-point function from [56]. The surface energy density is decomposed into contributions corresponding to the self-energy of the brane when the second brane is absent and the part induced by the second brane. The renormalization is required only for the first contribution. In the limit of infinite curvature radius, the result for parallel plates in the Minkowski bulk is recovered. Another special case with conformal relation to the Casimir problem in Minkowski spacetime corresponds to a conformally coupled massless field. The behavior of the SEMT in asymptotic regions of the parameters is discussed in Section 4. A numerical analysis for the induced surface energy density is presented as well. The main results of the paper are summarized in Section 5. The regularization of the self-energy contribution, by using the generalized zeta function approach, is considered in Appendix A. The finite part is separated on the basis of principal part prescription.

2. Geometry of the Problem

AdS spacetime is the maximally symmetric solution of the Einstein equations with a negative cosmological constant Λ as the only source of the gravitational field. In Poincaré coordinates $(t, x^1, \mathbf{x}, z)$, with t denoting the time, $\mathbf{x} = (x^2, \ldots, x^{D-1})$ the space coordinates with the spatial dimension $D > 1$, the corresponding metric tensor, g_{ik}, is given by

$$ds^2 = g_{ik}dx^i dx^k = \left(\frac{\alpha}{z}\right)^2 \left[dt^2 - \left(dx^1\right)^2 - d\mathbf{x}^2 - dz^2\right]. \tag{1}$$

Here, the parameter $\alpha = \sqrt{D(1-D)/(2\Lambda)}$ determines the curvature radius of the background spacetime, $-\infty < x^i < +\infty$ for $i, k = 0, 1, 2, \ldots, D-1$, and $0 \leq z < \infty$. The D-dimensional hypersurfaces $z = 0$ and $z = \infty$ present the AdS boundary and horizon, respectively. The proper distance along the z-direction is measured by the coordinate $y = \alpha \ln(z/\alpha)$, $-\infty < y < +\infty$. In the coordinate system $(t, x^1, \mathbf{x}, y)$ one has $g'_{DD} = 1$ and $g'_{ik} = g_{ik} = e^{-2y/\alpha}\eta_{ik}$, with η_{ik} being the metric tensor for Minkowski spacetime.

The aim is to investigate the surface Casimir densities induced by quantum fluctuations of a scalar field $\varphi(x)$ on codimension one parallel branes located at $x^1 = a_1$ and $x^1 = a_2$, $a_1 < a_2$ (see Figure 1 for the geometry of the problem). Throught the paper, it is assumed that the field is prepared in the Poincaré vacuum state. For a scalar field with curvature coupling parameter ξ, the corresponding field equation reads

$$\left(\Box + \xi R + m^2\right)\varphi(x) = 0, \tag{2}$$

where $\Box = g^{ik}\nabla_i\nabla_k$ is the covariant d'Alembertian, m is the mass, and $R = 2\Lambda(D + 1)/(D - 1)$ is the Ricci scalar for AdS spacetime. On the branes, the field operator is constrained by Robin boundary conditions,

$$(A_j + B_j n^i_{(j)}\nabla_i)\varphi(x) = 0, \ x^1 = a_j, \tag{3}$$

where $n^i_{(j)}$ is the normal to the brane at $x^1 = a_j$ pointing into the region under consideration. The branes divide the background space into three regions: $x^1 \leq a_1$, $a_1 \leq x^1 \leq a_2$, and $x^1 \geq a_2$. In the first and third regions, one has $n^i_{(1)} = -\delta^i_1 z/\alpha$ and $n^i_{(2)} = \delta^i_1 z/\alpha$, respectively, where δ^i_k is the Kronecker symbol. For the region $a_1 \leq x^1 \leq a_2$, the normal in Equation (3) is expressed as $n^i_{(j)} = (-1)^{j-1}\delta^i_1 z/\alpha$. In the discussion below, the region between the branes is considered. The VEVs for the regions $x^1 \leq a_1$ and $x^1 \geq a_2$ are obtained in the limits $a_2 \to \infty$ and $a_1 \to -\infty$. For the sets of the coefficients $(A_j, B_j) = (A_j, 0)$ and $(A_j, B_j) = (0, B_j)$ the constraints (3) are reduced to Dirichlet and Neumann boundary conditions, respectively. For Robin boundary conditions, here the special case $B_j/A_j = \alpha\beta_j/z$ is assumed, with β_j,

$j = 1, 2$, being constants. For this choice, the boundary conditions (3), written in terms of the coordinate $x^1_{(p)} = \alpha x^1 / z$, take the form

$$(1 + \beta_j n^1_{(j)} \partial_{x^1_{(p)}}) \varphi(x) = 0, \ x^1 = a_j, \tag{4}$$

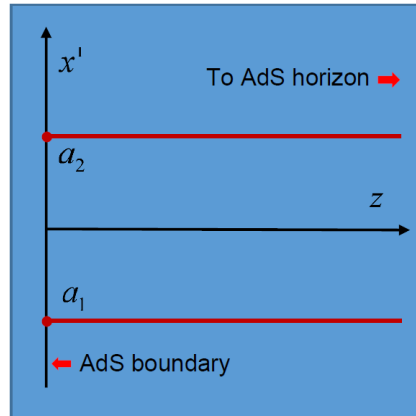where $\partial_a \equiv \partial / \partial a$.

Figure 1. The geometry of two branes orthogonal to the AdS boundary. See text for details.

The latter is the Robin boundary condition with constant coefficient β_j. This coefficient characterizes the properties of the brane and can be used to model the finite penetration length of quantum fluctuations. Note that the coordinate $x^1_{(p)}$ in Equation (4) measures the proper distance from the brane for a fixed z.

For the scalar field modes in the region between the branes, the eigenvalues of the quantum number k^1, corresponding to the momentum along the direction x^1, are quantized by the boundary conditions (4). Those eigenvalues are roots of the transcendental equation (see [56])

$$(\beta_1 + \beta_2) k^1 a \cos\left(k^1 a\right) + \left[\beta_1 \beta_2 (k^1)^2 - 1\right] \sin\left(k^1 a\right) = 0, \tag{5}$$

where $a = a_2 - a_1$. Depending on the values of the Robin coefficients, this equation, in addition to an infinite set of roots with real k^1, may have purely imaginary roots $k^1 = i\chi$ (for the corresponding conditions, see [60]). The energy of the scalar modes, with the momentum $\mathbf{k} = (k^2, \ldots, k^{D-1})$, $-\infty < k^i < +\infty$, $i = 2, \ldots, D-1$, in the subspace with coordinates $\mathbf{x}$, is expressed as $E = \sqrt{(k^1)^2 + \mathbf{k}^2 + \gamma^2}$, where $0 \leq \gamma < \infty$ is the quantum number corresponding to the z-direction. The dependence of the mode functions on the coordinate z is expressed in terms of the function $z^{D/2} J_\nu(\gamma z)$, with $J_\nu(u)$ being the Bessel function and

$$\nu = \sqrt{\frac{D^2}{4} - D(D+1)\xi + m^2 \alpha^2}. \tag{6}$$

Note that, in contrast to the Minkowski bulk, the energy of the scalar modes with given momentum does not depend on the mass of the field quanta. The mass enters in the problem through the parameter $\nu \geq 0$. Now, one can see that in the presence of imaginary roots $k^1 = i\chi$, for the scalar field modes with $\mathbf{k}^2 + \gamma^2 < \chi^2$, the energy becomes imaginary. This signals the instability of the vacuum state under consideration. In the discussion below, the values of the coefficients β_1 and β_2, for which there are no imaginary roots of the eigenvalue Equation (5), are assumed. The corresponding conditions read [60]

$$\beta_{1,2} \leq 0 \cup \{\beta_1 \beta_2 \leq 0, \beta_1 + \beta_2 > 1/a\}. \tag{7}$$

For a general $(D+1)$-dimensional spacetime with a smooth boundary ∂M_s, the SEMT $T_{ik}^{(s)}(x) = \tau_{ik}\delta(x; M_s)$, localized on the boundary by the one-sided Dirac delta function $\delta(x; M_s)$, is given by [57]

$$\tau_{ik} = (1/2 - 2\xi)h_{ik}\varphi n^l\nabla_l\varphi + \xi K_{ik}\varphi^2. \tag{8}$$

Here, $h_{ik} = g_{ik} + n_i n_k$ is the induced metric on the boundary, with n_i being the inward-pointing unit normal vector for M_s, and $K_{ik} = h_i^l h_k^m\nabla_l n_m$ is the corresponding extrinsic curvature tensor. The expression (8) was obtained in Ref. [57] by using the standard variational procedure for the action of a scalar field with general curvature coupling parameter and with an appropriate boundary term localized on M_s. Denoting the vacuum state by $|0\rangle$, the VEV of the SEMT is presented as

$$\langle 0|T_{ik}^{(s)}(x)|0\rangle = \delta(x; M_s)\langle 0|\tau_{ik}(x)|0\rangle, \tag{9}$$

where the VEV $\langle\tau_{ik}(x)\rangle \equiv \langle 0|\tau_{ik}(x)|0\rangle$ is written in terms of the Hadamard function $G^{(1)}(x, x') = \langle 0|\varphi(x)\varphi(x') + \varphi(x')\varphi(x)|0\rangle$ by the formula

$$\langle\tau_{ik}(x)\rangle = \frac{1}{2}\lim_{x'\to x}\left[(1/2 - 2\xi)h_{ik}n^l\nabla_l + \xi K_{ik}\right]G^{(1)}(x, x'). \tag{10}$$

The limit contains two types of divergences. The first type of the divergences is present already in the case when the point x does not belong to the boundary. The corresponding divergent part is the same as that in the problem where the branes are absent and is removed by the subtraction from the Hadamard function in Equation (10), the corresponding function in the brane-free geometry. The SEMT is absent in the latter geometry and the brane-free Hadamard function does not contribute to the VEV of the SEMT. The second type of divergences originates from the surface divergences in quantum field theory with boundaries and arises when the point x belongs to the boundary.

3. VEV of the SEMT

3.1. General Expression

In the problem under consideration, and for the region $a_1 \leq x^1 \leq a_2$, the inward-pointing normal is given by $n_i = n_{(j)i} = (-1)^j\delta_i^1\alpha/z$ for the brane at $x^1 = a_j$. The corresponding induced metric reads $h_{ik} = g_{ik}$, $i, k \neq 1$, and $h_{11} = 0$. Now, it can be immediately checked that the extrinsic curvature tensor for the branes vanishes, $K_{ik} = 0$. Hence, the VEV of the SEMT is expressed as

$$\langle\tau_{ik}(x)\rangle = \left(\frac{1}{4} - \xi\right)h_{ik}n^l\lim_{x'\to x}\nabla_l G^{(1)}(x, x'). \tag{11}$$

The expression for the Hadamard function in the region between the branes is obtained from the corresponding expression for the Wightman function derived in Ref. [56]. The Wightman function is presented in the decomposed form

$$
\begin{aligned}
G^{(1)}(x, x') =\ & G_j^{(1)}(x, x') + \frac{2(zz')^{D/2}}{(2\pi\alpha)^{D-1}}\int d\mathbf{k}\, e^{i\mathbf{k}\Delta\mathbf{x}}\int_0^\infty d\gamma\, \gamma J_\nu(\gamma z)J_\nu(\gamma z') \\
& \times \int_w^\infty d\lambda\, \frac{\cosh(\sqrt{\lambda^2 - w^2}\Delta t)}{\sqrt{\lambda^2 - w^2}}\frac{2\cosh\left[\lambda(x^1 - x'^1)\right] + \sum_{l=\pm 1}\left[e^{|x^1 + x'^1 - 2a_j|\lambda}c_j(\lambda)\right]^l}{c_1(\lambda)c_2(\lambda)e^{2a\lambda} - 1},
\end{aligned}
\tag{12}
$$

where $\Delta\mathbf{x} = \mathbf{x} - \mathbf{x}'$, $w = \sqrt{\gamma^2 + k^2}$, $k = |\mathbf{k}|$, J_ν is the Bessel function, and

$$c_j(\lambda) = \frac{\beta_j\lambda - 1}{\beta_j\lambda + 1}. \tag{13}$$

In Equation (12),

$$
\begin{aligned}
G_j^{(1)}(x, x') \;=\;& G_0^{(1)}(x, x') + \frac{(zz')^{D/2}}{(2\pi\alpha)^{D-1}} \int d\mathbf{k}\, e^{i\mathbf{k}\Delta\mathbf{x}} \int_0^\infty d\gamma\, \gamma J_\nu(\gamma z) J_\nu(\gamma z') \\
&\times \int_0^\infty d\lambda\, \frac{e^{-i\sqrt{\lambda^2+w^2}\,\Delta t}}{\sqrt{\lambda^2+w^2}} \sum_{l=\pm 1} \left[e^{i|x^1+x'^1-2a_j|\lambda} c_j(i\lambda) \right]^l,
\end{aligned}
\tag{14}
$$

is the Hadamard function in the problem with a brane at $x^1 = a_j$ when the second brane is absent. Again, it is obtained from the corresponding Wightman function given in Refs. [55,56]. The first term in the right-hand side, $G_0^{(1)}(x, x')$, is the Hadamard function in AdS spacetime without branes. The last term in Equation (12) is interpreted as the contribution to the Hadamard function in the region $a_1 \le x^1 \le a_2$, induced by the brane at $x^1 = a_{j'}$ when this term is added to the problem with a single brane at $x^1 = a_j$. Here, and below, $j' = 1$ for $j = 2$ and $j' = 2$ for $j = 1$.

Combining (11) and (12), the SEMT on the brane at $x^1 = a_j$ is decomposed as

$$
\langle \tau_{ik} \rangle_j = \langle \tau_{ik} \rangle_j^{(0)} + \langle \tau_{ik} \rangle_j^{\text{ind}}.
\tag{15}
$$

Here, $\langle \tau_{ik} \rangle_j^{(0)}$ is the VEV of the SEMT when the second brane is absent and $\langle \tau_{ik} \rangle_j^{\text{ind}}$ is induced by the second brane at $x^1 = a_{j'}$. The VEV $\langle \tau_{ik} \rangle_j^{(0)}$ is obtained from Equation (11) with the Hadamard function (14). By taking into account that in the AdS spacetime without branes the SEMT is absent, one obtains:

$$
\langle \tau_i^k \rangle_j^{(0)} = (4\xi - 1) \frac{\delta_i^k \beta_j z^{D+1}}{(2\pi)^{D-1}\alpha^D} \int d\mathbf{k} \int_0^\infty d\gamma\, \gamma J_\nu^2(\gamma z) \int_0^\infty d\lambda\, \frac{1}{\sqrt{\lambda^2+b^2}} \frac{\lambda^2}{1+\lambda^2\beta_j^2}.
\tag{16}
$$

The vacuum SEMT induced by the second brane comes from the last term in Equation (12). It is presented in the form

$$
\begin{aligned}
\langle \tau_i^k \rangle_j^{\text{ind}} \;=\;& (4\xi - 1) \frac{2\delta_i^k \beta_j z^{D+1}}{(2\pi)^{D-1}\alpha^D} \int d\mathbf{k} \int_0^\infty d\gamma\, \gamma J_\nu^2(\gamma z) \int_b^\infty d\lambda\, \frac{\lambda^2}{\sqrt{\lambda^2-b^2}} \\
&\times \frac{\beta_{j'}\lambda + 1}{\beta_j\lambda - 1} \frac{1}{(\beta_1\lambda - 1)(\beta_2\lambda - 1)e^{2a\lambda} - (\beta_1\lambda + 1)(\beta_2\lambda + 1)}.
\end{aligned}
\tag{17}
$$

The expression (16) for the self-SEMT is divergent and needs a regularization with a subsequent renormalization removing the divergences. This type of surface divergence is well known in quantum field theory with boundaries.

Note that for an observer living on the brane $x^1 = a_j$, the D-dimensional line element is obtained from Equation(1), taking $dx^1 = 0$. It describes D-dimensional AdS spacetime generated by a cosmological constant $\Lambda' = (1 - 2/D)\Lambda$. From the point of view of an observer on the brane, the energy–momentum tensor $\langle \tau_i^k \rangle_j$ is a source of gravitation, with the energy density $\varepsilon_j = \langle \tau_0^0 \rangle_j$ and isotropic effective pressure $p_j = -\langle \tau_2^2 \rangle_j = \cdots = -\langle \tau_D^D \rangle_j$. The corresponding equation of state reads $p_j = -\varepsilon_j$, hence $\langle \tau_i^k \rangle_j$ is a source of the cosmological constant type. Certainly, the latter property is a consequence of the symmetry in the problem under consideration. In accordance with Equation (15), the surface energy density is decomposed into the self-energy and the contribution induced by the second brane:

$$
\varepsilon_j = \varepsilon_j^{(0)} + \varepsilon_j^{\text{ind}},
\tag{18}
$$

where $\varepsilon_j^{\text{ind}} = \langle \tau_0^0 \rangle_j^{\text{ind}}$.

The regularization of the divergent expression on the right-hand side of Equation (16), based on the generalized zeta function approach, is discussed in Appendix A. The expres-

sion is decomposed into pole and finite contributions obtained from Equation (A15) in combination with Equation (A2). In the principal part prescription the finite self-energy, $\varepsilon_j^{(0)}$ is identified with the finite part of the corresponding Laurent expansion near the physical point $s = 1$. In order to remove the divergent part, to note is that the VEV $\langle \tau_{ik} \rangle_j$ is a part of a theory which contains other contributions localized on the brane and the divergences in $\langle \tau_{ik} \rangle_j$ are absorbed by renormalizing the parameters in those contributions. The finite part of the SEMT $\langle \tau_{ik} \rangle_j^{(0)}$ is given by Equation (A19). This part contains renormalization ambiguities, which can be fixed by imposing additional renormalization conditions. Here, the situation is completely parallel to that for the case of the total Casimir energy discussed, for example, in Ref. [4]. Similar to Equation (15), the Casimir energy for a system composed of separate bodies is decomposed into the self-energies and the interaction energy. The renormalization is required only for the self-energies.

Unlike the self-energy part, $\varepsilon_j^{(0)}$, the surface energy density, $\varepsilon_j^{\text{ind}}$, and the related SEMT, $\langle \tau_i^k \rangle_j^{\text{ind}}$, are finite and uniquely defined. The main concern in the discussion below is that part of the energy–momentum tensor. Integrating over the angular coordinates of **k** and introducing the polar coordinates in the plane (k, u), one integrates over the related polar angle:

$$
\begin{aligned}
\langle \tau_i^k \rangle_j^{\text{ind}} &= \frac{(4\xi - 1)\delta_i^k \beta_j z^{D+1}}{2^{D-2}\pi^{\frac{D-1}{2}}\Gamma(\frac{D-1}{2})\alpha^D} \int_0^\infty d\gamma\, \gamma J_\nu^2(\gamma z) \int_0^\infty dr\, r^{D-2} \frac{\beta_{j'}\lambda + 1}{\beta_j \lambda - 1} \\
&\quad \times \left. \frac{\lambda}{(\beta_1\lambda - 1)(\beta_2\lambda - 1)e^{2a\lambda} - (\beta_1\lambda + 1)(\beta_2\lambda + 1)} \right|_{\lambda = \sqrt{\gamma^2 + r^2}}.
\end{aligned}
\tag{19}
$$

Next, let us introduce polar coordinates in the plane (γ, r). The angular integral is evaluated by using the result [61]

$$
\int_0^1 dx\, x(1 - x^2)^{\frac{D-3}{2}} J_\nu^2(ux) = \frac{\Gamma(\frac{D-1}{2})}{2^{2\nu+1}} u^{2\nu} F_\nu(u),
\tag{20}
$$

with the function

$$
F_\nu(u) = \frac{{}_1F_2(\nu + \frac{1}{2}; \frac{D+1}{2} + \nu, 1 + 2\nu; -u^2)}{\Gamma(\frac{D+1}{2} + \nu)\Gamma(1 + \nu)}.
\tag{21}
$$

Here, Γ is the gamma function and ${}_1F_2(a; b, c; x)$ is the hypergeometric function. This gives:

$$
\langle \tau_i^k \rangle_j^{\text{ind}} = \frac{(4\xi - 1)\delta_i^k \beta_j z^{D+2\nu+1}}{2^{D+2\nu-1}\pi^{\frac{D-1}{2}}\alpha^D} \int_0^\infty d\lambda\, \frac{\beta_{j'}\lambda + 1}{\beta_j\lambda - 1} \frac{\lambda^{D+2\nu+1} F_\nu(\lambda z)}{(\beta_1\lambda - 1)(\beta_2\lambda - 1)e^{2a\lambda} - (\beta_1\lambda + 1)(\beta_2\lambda + 1)}.
\tag{22}
$$

From this it follows that the induced SEMT on the brane $x^1 = a_j$ vanishes for special cases of Dirichlet and Neumann boundary conditions on that brane. Depending on the coefficients β_j and on the separation between the branes, the induced energy density $\varepsilon_j^{\text{ind}}$ can be either positive or negative (see numerical examples below). Introducing a new integration variable $u = \lambda z$, one can see that the product $\alpha^D \langle \tau_i^k \rangle_j^{\text{ind}}$ depends on the quantities z, a_j, β_j, having dimension of length, in the form of two dimensionless ratios a/z, β_j/z. Those ratios are the proper values of the quantities, measured by an observer with fixed z, in units of the curvature radius α. This feature is a consequence of the AdS maximal symmetry.

3.2. Minkowskian Limit and a Conformally Coupled Massless Field

To clarify the features of the SEMT on the branes, let us consider special cases and asymptotic regions of the parameters. First, let us discuss the Minkowskian limit corresponding to $\alpha \to \infty$ for fixed coordinate y. For the coordinate z, in the leading or-

der, one has $z \approx \alpha$ and the line element (1) tends to the Minkowskian interval $ds_M^2 = dt^2 - (dx^1)^2 - d\mathbf{x}^2 - dy^2$. The geometry of the corresponding problem consists of two parallel plates at $x^1 = a_1$ and $x^1 = a_2$ with the boundary condition $(1 - (-1)^j \beta_j \partial_1) \varphi(x) = 0$ at $x^1 = a_j$ in the region $a_1 \leq x^1 \leq a_2$; here, $\partial_1 \equiv \partial/\partial_{x^1}$. For relatively large values of α and for a massive field, the parameter ν is large, $\nu \approx m\alpha$, and one needs the asymptotic of the function $F_\nu(\lambda z)$ when both the argument and the order are considerably large. The corresponding analysis in Ref. [55] shows that the function $F_\nu(\nu\lambda/m)$ is exponentially suppressed for $\nu \gg 1$ and $\lambda < m$. For $\lambda > m$, the leading behavior is approximated by [55]

$$F_\nu\left(\frac{\nu}{m}\lambda\right) \approx \frac{(\lambda^2 - m^2)^{D/2-1}(2m/\nu)^{2\nu+1}}{2\sqrt{\pi}\Gamma(\frac{D}{2})\lambda^{D+2\nu-1}}. \tag{23}$$

By using this asymptotic for the part of the integral in Equation (22) over the region $m \leq \lambda < \infty$, one obtains the SEMT on the plate $x^1 = a_j$ in Minkowski spacetime, $\langle \tau_i^k \rangle_{(M)j}^{\text{ind}} = \lim_{\alpha \to \infty} \langle \tau_i^k \rangle_j^{\text{ind}}$, given by

$$\langle \tau_i^k \rangle_{(M)j}^{\text{ind}} = \frac{(4\xi - 1)\delta_i^k \beta_j}{2^{D-1}\pi^{D/2}\Gamma(\frac{D}{2})} \int_m^\infty d\lambda \frac{\beta_{j'}\lambda + 1}{\beta_j\lambda - 1} \frac{\lambda^2(\lambda^2 - m^2)^{D/2-1}}{(\beta_1\lambda - 1)(\beta_2\lambda - 1)e^{2a\lambda} - (\beta_1\lambda + 1)(\beta_2\lambda + 1)}. \tag{24}$$

This result for a massive field was obtained in Ref. [58] as a limiting case of the problem with two branes in AdS spacetime parallel to the AdS boundary. In the case of a massless field, the expression for $\langle \tau_i^k \rangle_{(M)1}^{\text{ind}} + \langle \tau_i^k \rangle_{(M)2}^{\text{ind}}$, obtained from Equation (24), coincides with the result derived in Ref. [60]. The VEV of the SEMT for a single Robin boundary in background of $(3 + 1)$-dimensional Minkowski spacetime has also been considered in Refs. [62,63].

In the case of a massless field with conformal coupling, one has $\xi = \xi_D = \frac{D-1}{4D}$ and $\nu = 1/2$. By taking into account that $J_{1/2}(x) = \sqrt{\frac{\pi}{2x}} \sin x$, from Equation (20) one obtains [55]:

$$F_{1/2}(u) = \frac{2}{\sqrt{\pi}u^2}\left[\frac{1}{\Gamma(\frac{D}{2})} - \frac{J_{\frac{D}{2}-1}(2u)}{u^{\frac{D}{2}-1}}\right]. \tag{25}$$

Substituting this expression into Equation (22) one obtains

$$\varepsilon_j^{\text{ind}} = (z/\alpha)^D \varepsilon_{(M)j}^{\text{ind}}, \tag{26}$$

with

$$\begin{aligned}
\varepsilon_{(M)j}^{\text{ind}} &= -\frac{2^{1-D}\beta_j}{D\pi^{\frac{D}{2}}}\int_0^\infty d\lambda \frac{\beta_{j'}\lambda + 1}{\beta_j\lambda - 1}\left[\frac{1}{\Gamma(\frac{D}{2})} - \frac{J_{\frac{D}{2}-1}(2\lambda z)}{(\lambda z)^{D/2-1}}\right] \\
&\quad \times \frac{\lambda^D}{(\beta_1\lambda - 1)(\beta_2\lambda - 1)e^{2a\lambda} - (\beta_1\lambda + 1)(\beta_2\lambda + 1)}.
\end{aligned} \tag{27}$$

For a conformally coupled massless scalar field, the problem considered here is conformally related to the problem of two Robin plates at $x^1 = a_j$, $j = 1, 2$, in Minkowski spacetime, described by the interval $ds_M^2 = dt^2 - (dx^1)^2 - d\mathbf{x}^2 - dz^2$, intersected by a Dirichlet plate located at $z = 0$. The presence of the latter is related to the boundary condition for scalar field modes imposed on the AdS boundary $z = 0$. The surface energy density (27) is induced on the plate $x^1 = a_j$ by the presence of the second plate $x^1 = a_{j'}$. The part of $\varepsilon_{(M)j}^{\text{ind}}$ coming from the first term in the square brackets is the corresponding quantity in the geometry where the plate $z = 0$ is absent (see Equation (24) for $m = 0$). The part with the second term is a consequence of the presence of the plate $z = 0$. Note that

$\varepsilon_{(M)j}^{ind}$ vanishes on that plate: $\varepsilon_{(M)j}^{ind}|_{z=0} = 0$. This is a consequence of Dirichlet boundary conditions at $z = 0$.

4. Asymptotics and Numerical Analysis

In this Section, the behavior of the VEV for SEMT in asymptotic regions of the parameters is studied. Let us start with the asymptotics at relatively small and large separations between the branes. For a given z, the proper separation between the branes is given by $a_{(p)} = \alpha a/z$. For quite small proper separations compared to the curvature radius, one has $a/z \ll 1$ and the integral in Equation (22) is dominated by the contribution of the region with large enough values of the argument of the function $F_\nu(\lambda z)$. By using the corresponding asymptotic [55],

$$F_\nu(u) \approx \frac{2^{2\nu}}{\sqrt{\pi}\Gamma\left(\frac{D}{2}\right)u^{2\nu+1}}, \quad u \gg 1, \tag{28}$$

one can see that the relation

$$\langle \tau_i^k \rangle_j^{ind} \approx (z/\alpha)^D \langle \tau_i^k \rangle_{(M)j}^{ind}|_{m=0}, \tag{29}$$

takes place, where $\langle \tau_i^k \rangle_{(M)j}^{ind}|_{m=0}$ is given by Equation (24) with $m = 0$. In the limit under consideration, the main contribution to the SEMT comes from the zero-point fluctuations with wavelengths smaller than the curvature radius and the effect of the gravitational field is weak. The asymptotic (29) is further simplified if the separation a is smaller than the length scales determined by the boundary conditions, $a/|\beta_l| \ll 1$, $l = 1, 2$. For Dirichlet boundary conditions on the brane $x^1 = a_{j'}$, $\beta_{j'} = 0$, the condition $a/|\beta_j| \ll 1$ is assumed. Under those conditions, $\lambda|\beta_l| \gg 1$ ($\lambda|\beta_j| \gg 1$ in the case $\beta_{j'} = 0$) for the region of λ that dominates in the integral on the right-hand side of Equation (24) (with $m = 0$). In the leading order one obtains:

$$\langle \tau_i^k \rangle_j^{ind} \approx \delta_i^k \frac{(z/\alpha)^D (4\xi - 1)}{2^D \pi^{\frac{D+1}{2}} a^{D-1}} \zeta(D-1)\Gamma\left(\frac{D-1}{2}\right) \begin{cases} 1/\beta_{j'}, & \beta_{j'} \neq 0 \\ (2^{2-D} - 1)/\beta_j, & \beta_{j'} = 0 \end{cases}, \tag{30}$$

with $\zeta(u)$ being the Riemann zeta function. Note that the asymptotic (29) also describes the behavior of the SEMT near the AdS horizon. As is seen from Equation (30), in the special cases of minimally ($\xi = 0$) and conformally ($\xi = \xi_D$) coupled fields and for quite small separations between the branes, the energy density induced on the brane $x^1 = a_j$ by the second brane is positive for $\beta_{j'} < 0$ and negative for $\beta_{j'} > 0$. For the Dirichlet boundary condition on the second brane ($\beta_{j'} = 0$), the sign of the induced energy density coincides with the sign of the product $(1 - 4\xi)\beta_j$.

In the opposite limit of considerably large proper separations compared with the curvature radius, one has $a/z \gg 1$ and the main contribution to the integral in Equation (22) gives the region near the lower limit, corresponding to $\lambda z \ll 1$. In the leading order, replacing the function $F_\nu(\lambda z)$ by

$$F_\nu(0) = \frac{1}{\Gamma(\nu+1)\Gamma\left(\frac{D+1}{2} + \nu\right)}, \tag{31}$$

one obtains

$$\langle \tau_i^k \rangle_j^{ind} \approx \frac{8(4\xi - 1)\delta_i^k (z/2)^{D+2\nu+2} \beta_j/z}{\pi^{\frac{D-1}{2}}\Gamma(\nu+1)\Gamma\left(\frac{D+1}{2} + \nu\right)\alpha^D} \int_0^\infty d\lambda \frac{\lambda \beta_{j'} + 1}{\lambda \beta_j - 1} \frac{\lambda^{D+2\nu+1}}{(\lambda \beta_1 - 1)(\lambda \beta_2 - 1)e^{2\lambda a} - (\lambda \beta_1 + 1)(\lambda \beta_2 + 1)}. \tag{32}$$

This expression is further simplified for separations larger than the length scales in Robin boundary conditions. Assuming $a \gg |\beta_l|$, $l = 1, 2$, one can see that $\lambda|\beta_l| \ll 1$ for the

region, giving the dominant contribution to the integral in Equation (32). For the case of Neumann boundary conditions on the brane $x^1 = a_{j'}$, corresponding to the limit $|\beta_j| \to \infty$, for separations $a \gg |\beta_j|$, one has $\lambda|\beta_j| \ll 1$ in the region with the dominant contribution to the integral. For the leading order term in the VEV of the SEMT and for non-Neumann ($A_j \neq 0$) boundary conditions on the second brane, one finds:

$$\langle \tau_i^k \rangle^{\text{ind}} \approx \delta_i^k \frac{(1 - 4\xi)\zeta(D + 2\nu + 2)\beta_j/a}{\pi^{\frac{D}{2}}\Gamma(\nu + 1)\alpha^D(2a/z)^{D+2\nu+1}} (D + 2\nu + 1)\Gamma\left(\frac{D}{2} + \nu + 1\right). \tag{33}$$

For Neumann boundary conditions on the second brane, an additional factor $(2^{-D-2\nu-1} - 1)$ should be added to the right-hand side of Equation (33). One can see that at considerably large distances between the branes the decay of the SEMT, as a function of the proper separation, is a power law for both massive and massless fields. This feature for massive fields is in contrast with the corresponding behavior for parallel plates in the Minkowski bulk, where the suppression is exponential, by the factor e^{-2ma}. Let us note that the Formula (32) also gives the asymptotic of the SEMT near the AdS boundary. As seen, for fixed β_j, the SEMT tends to zero on the AdS boundary, like $z^{D+2\nu+1}$. The asymptotic estimate (33) shows that for $\beta_j < 0$, and for non-Neumann boundary conditions on the second brane ($1/\beta_{j'} \neq 0$), at quite large separations between the branes the induced energy density $\varepsilon_j^{\text{ind}}$ is negative for minimally and conformally coupled fields.

Figure 2 presents the VEV of the energy density, induced on the brane at $x^1 = a_1$ by the brane at $x^1 = a_2$ as a function of the proper separation between the branes a/z. The graphs are plotted for a scalar field in $(4 + 1)$-dimensional AdS spacetime ($D = 4$), for the Robin boundary condition with $\beta_1/z = -0.5$ and with the mass corresponding to $m\alpha = 0.5$. The dependence on the proper separation is displayed for different values of the ratio β_2/z (the numbers near the curves) and for Dirichlet and Neumann boundary conditions on the second brane. Figure 2, left, and Figure 2, right, correspond to conformally and minimally coupled fields, respectively. In accordance with the asymptotic analysis given above, for minimally and conformally coupled fields and at relatively small separations between the branes, the energy density, induced by the second brane, is positive (negative) for non-Dirichlet (Dirichlet) boundary conditions on the second brane. At considerably large separations, the energy density is negative for non-Neumann boundary conditions on the second brane and is positive for Neumann boundary conditions. The inset in Figure 2, right, is given to emphasize the change in the sign of the surface energy density as a function of the separation between the branes.

In Figure 3, for conformally (Figure 3, left) and minimally (Figure 3, right) coupled scalar fields in $D = 4$ spatial dimensions, the dependence of the energy density $\varepsilon_1^{\text{ind}}$ on the Robin coefficient β_1/z is plotted for different values of the Robin coefficient β_2/z (the numbers marking the curves) on the second brane and for Dirichlet and Neumann boundary conditions. The graphs are plotted for $m\alpha = 0.5$ and $a/z = 1$.
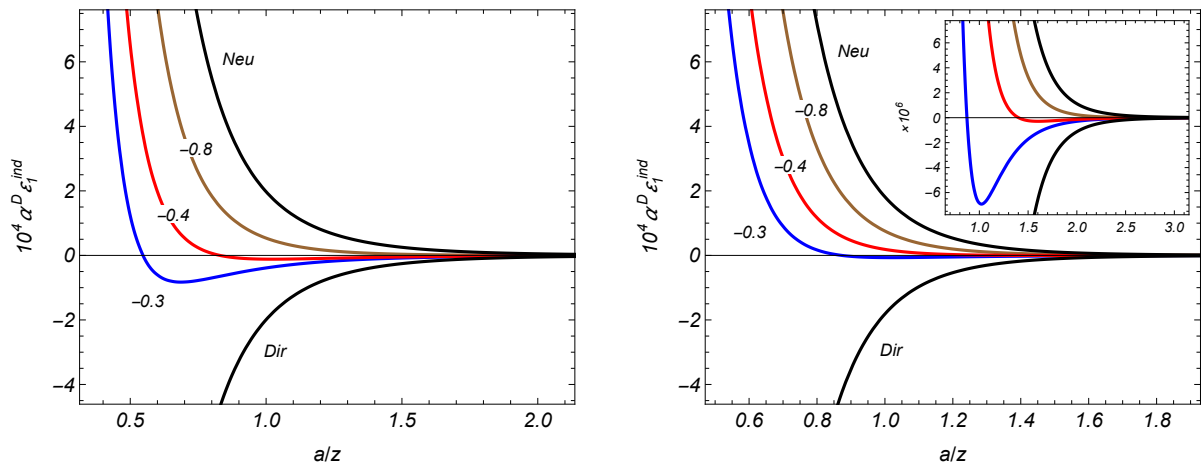
Figure 2. The induced surface energy density on the brane for conformally (**left**) and minimally (**right**) coupled fields at $x^1 = a_1$, in units of α^{-D}, versus the proper separation between the branes for $D = 4$, $m\alpha = 0.5$, and $\beta_1/z = 0.5$. The graphs are presented for different values of the ratio β_2/z (the numbers marking the curves) and for Dirichlet (marked "Dir") and Neumann ("Neu") boundary conditions on the second brane ($\beta_2/z = 0$ and $\beta_2/z = \infty$, respectively). See text for details.
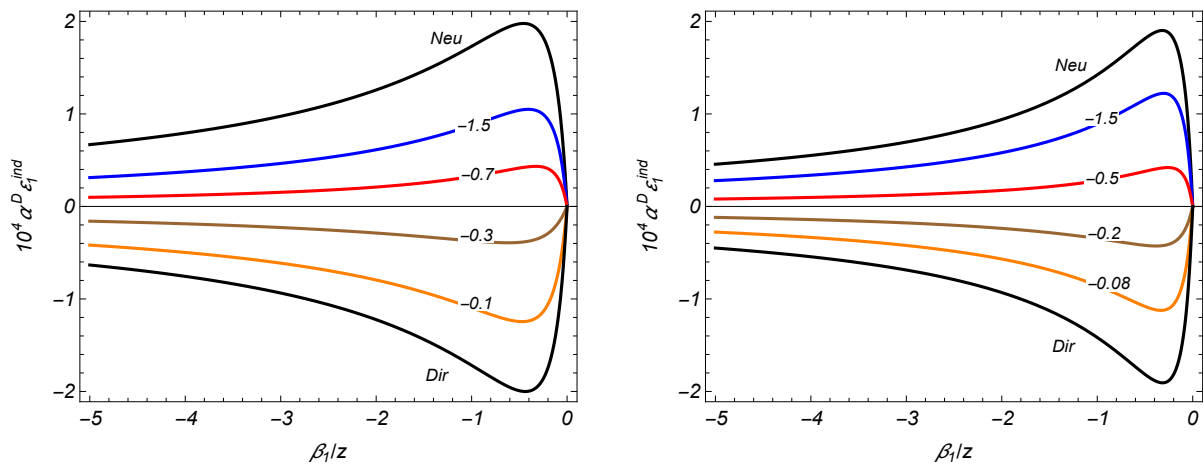

Figure 3. The induced surface energy density on the brane for conformally (**left**) and minimally (**right**) coupled fields at $x^1 = a_1$ for $D = 4$, $m\alpha = 0.5$, and $a/z = 1$ versus the Robin coefficient β_1/z for different values of β_2/z (the numbers marking the curves), $\beta_2/z = 0$ and $\beta_2/z = -\infty$ for Dirichlet (marked "Dir") and Neumann ("Neu") boundary conditions. See text for details.

The dependence of the surface energy density on the mass of the field (in units of $1/\alpha$) is displayed in Figure 4 for conformally (Figure 4, left) and minimally (Figure 4, right) coupled scalar fields in spatial dimensions $D = 4$. The graphs are plotted for $a/z = 1$, $\beta_1/z = -0.5$, and for different values of the ratio β_2/z (the numbers marking the curves). The graphs corresponding to Robin boundary conditions, $-\infty < \beta_2/z < 0$, are located between the graphs corresponding to Neumann and Dirichlet boundary conditions on the second brane ($\beta_2/z = -\infty$ and $\beta_2/z = 0$, respectively). As seen, the induced energy density, in general, is not a monotonic function of the field mass. In addition, for fixed values of the other parameters it may change the sign as a function of the mass. In particular, that is the case for a minimally coupled field with the boundary conditions corresponding to $\beta_1/z = -0.5$ and $\beta_2/z = -0.25$ (see Figure 4, right).
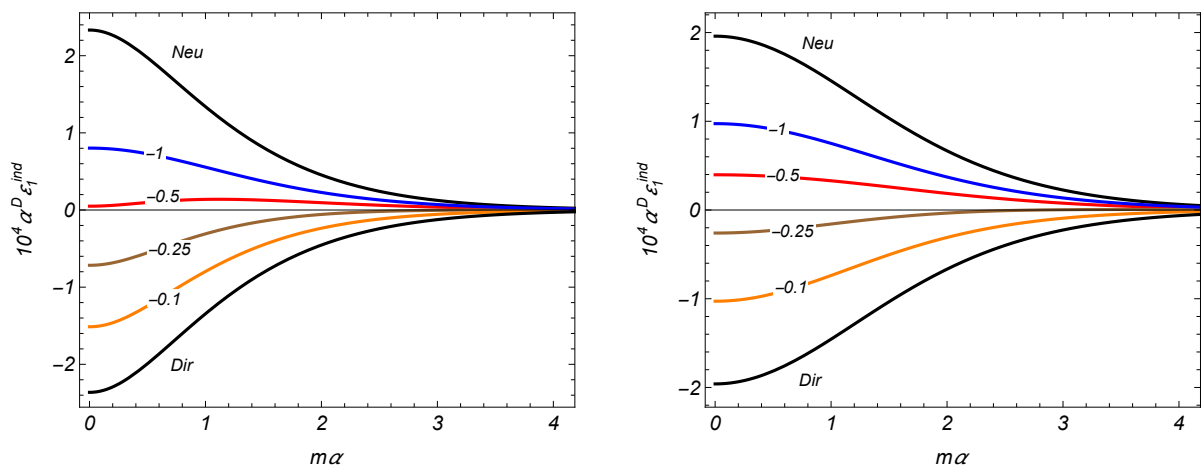
Figure 4. The dependence of the surface energy density on the first brane, induced by the second brane for conformally (**left** and minimally **right** coupled fields versus the field mass for $D = 4$, $a/z = 1$, $\beta_1/z = -0.5$ and for separate values of β_2/z (the numbers marking the curves). The graphs for Dirichlet (marked "Dir") and Neumann ("Neu") boundary conditions on the second brane are presented as well. See text for details.

5. Conclusions

For a scalar field with general curvature coupling, the VEV of the SEMT induced on branes in AdS spacetime orthogonal to its boundary has been studied. On the branes, the field operator is constrained by the boundary conditions (3) or, equivalently, by the conditions (4). To ensure the stability of the vacuum state, the values of the parameters in Robin boundary conditions are restricted by (7). For the geometry of the branes under consideration, the extrinsic curvature tensor is zero and the general formula for the SEMT is simplified to Equation (11). From the viewpoint of observers living on the branes this SEMT presents a gravitational source with the equation of state for a cosmological constant. In order to evaluate the corresponding VEV, the Hadamard function is used, obtained from the positive frequency Wightman function from Ref. [56]. In the region between the branes, the Hadamard function is decomposed into single-brane and the second-brane-induced contributions. This allows the separation of the part generated by the second brane from the total VEV of the SEMT. The surface divergences are contained in the self-energy contributions on the branes and the renormalization is required for those parts only. In order to extract the finite parts in the corresponding VEVs, in Appendix A, the regularization procedure based on the generalized zeta function approach is employed. The divergences, appearing in the form of simple poles, are absorbed by the renormalization of the corresponding parameters in the "classical" action localized on the branes. The finite part of the SEMT separated in this way contains renormalization ambiguities and additional conditions are required to obtain a unique result. This is fully similar to the case of the self-energy in the Casimir effect in the geometry of a single boundary (see, for example, the corresponding discussion in Ref. [4]).

The part of the SEMT induced on the brane by the presence of the second brane is finite and uniquely defined. The induced SEMT on the brane $x^1 = a_j$ is given by the expression (22). It vanishes for special cases of Dirichlet and Neumann boundary conditions on that brane. As a consequence of the maximal symmetry of AdS spacetime, for the general case of Robin boundary conditions, the dimensionless quantity $\alpha^D \langle \tau_i^k \rangle_j^{\text{ind}}$ is completely determined by the dimensionless ratios a/z and β_j/z, $j = 1, 2$. The first one is the proper separation between the branes, measured by an observer with fixed z in units of the curvature radius α. The VEV of the SEMT for Robin parallel plates in the Minkowski bulk is obtained from Equation (22) in the limit $\alpha \to \infty$ and is expressed as Equation (24). The latter includes special cases previously discussed in the literature and coincides with the result obtained in Ref. [58] as a limit $\alpha \to \infty$ of the SEMT in the geometry of branes

parallel to the AdS boundary. For a conformally coupled massless field, the problem in the AdS bulk is conformally related to the problem in Minkowski spacetime consisting of two parallel Robin plates perpendicularly intersected by a Dirichlet plate, the latter being the image of the AdS boundary. The VEV in the Minkowski counterpart is given by the Formula (27), where the contribution of the Dirichlet plate comes from the term in the square brackets with the Bessel function.

At quite small separations between the branes, compared to the curvature radius and length scales determined by the Robin coefficients, the influence of the gravitational field on the SEMT is small enough and the leading term in the corresponding expansion is expressed by Equation (30). In this limit, and for non-Dirichlet (Dirichlet) boundary conditions on the brane $x^1 = a_{j'}$, the sign of the surface energy density induced on the brane $x^1 = a_j$ coincides with the sign of the product $(4\xi - 1)\beta_{j'}$ $((1 - 4\xi)\beta_j)$. The effects of the gravitational field are essential at proper separations between the branes of the order or larger than the curvature scale of the background geometry. Additionally, assuming that the separation is larger than the length scales fixed by the boundary conditions, the leading behavior of the induced SEMT is described by Equation (33) for non-Neumann boundary conditions on the second brane. The sign of the energy density coincides with the sign of $(1 - 4\xi)\beta_j$. For Neumann conditions on the second brane, an additional factor $(2^{-D-2\nu-1} - 1)$ needs to be added on the right-hand side of Equation (33) and the energy density at quite large distances has an opposite sign. An important feature of the large-distance behavior of the SEMT is the power law decay as a function of the proper separation. For parallel plates in Minkowski spacetime, the corresponding decay for massive fields is exponential. The induced surface energy density vanishes on the AdS boundary like $z^{D+2\nu+1}$ and behaves as $(z/\alpha)^D$ near the AdS horizon.

The investigations of the brane-induced effects on the properties of the scalar vacuum in AdS spacetime have discussed the branes parallel or perpendicular to the AdS boundary. An interesting generalization, that includes these special cases, would be the geometry of branes crossing the AdS boundary at an arbitrary angle. In this case, the dependence of the scalar mode functions on the coordinates parallel and perpendicular to the AdS boundary are not separable and the problem is more complicated. It is expected that for a general crossing angle, in addition the normal and shear Casimir forces, a rotational momentum to appear generated by the vacuum fluctuations.

The study of the boundary-induced effects on the fermionic and electromagnetic vacua for branes perpendicular to the AdS boundary is another direction for further research. The dependence of the mode functions on the coordinate z is expressed in terms of the functions $J_{m\alpha \pm 1/2}(\gamma z)$ for the fermionic field (with m being the mass of the field) and in terms of the function $J_{D/2-1}(\gamma z)$ for the vector potential of the electromagnetic field. Similar to the case of a scalar field, it is expected that the equation determining the eigenvalues of the quantum number corresponding to the direction normal to the branes to be the same as that in the Minkowski bulk, with the same boundary conditions on planar boundaries. The summation over those eigenvalues in the corresponding mode sum for the VEV of the energy–momentum tensor can be achieved using the generalized Abel–Plana formula. This allows the explicit extraction of the brane-induced contribution. Note that previous investigations of the vacuum energy–momentum tensor for fermionic and electromagnetic fields have considered branes parallel to the AdS boundary (see [41–45]). The bag boundary condition has been imposed for the fermionic field, and for the electromagnetic field, the perfect conductor and confining boundary conditions have been discussed.

Data Availability Statement: Data are contained within the article.

Conflicts of Interest: The author declares no conflict of interest.

Appendix A. Surface Densities for a Single Brane

It was shown above that the VEV of the SEMT for a single brane at $x^1 = a_j$ is presented in the form (16). The corresponding expression is divergent and can be regularized by using the generalized zeta function approach (for a general introduction and applications in the theory of the Casimir effect, see, e.g., [64–66]). Let us consider the function

$$F(s,z) = \frac{\mu^{s-1}\beta_j z^{D+1}}{(2\pi)^{D-1}} \int_0^\infty d\gamma\, \gamma J_\nu^2(\gamma z) \int_0^\infty d\lambda\, \lambda^2 \int d\mathbf{k}\, \frac{(\lambda^2 + \gamma^2 + k^2)^{-\frac{s}{2}}}{1 + \lambda^2 \beta_j^2}, \qquad (A1)$$

with, in general, complex argument s. As seen below, the expression on the right-hand side is finite for $\mathrm{Re}\, s > D$. The scale parameter μ, having dimension of inverse length, is introduced to keep the function $F(s,z)$ dimensionless. Following the principal part prescription, considered previously in the literature for the total Casimir energy in ultrastatic manifolds with boundaries (see [64,65,67]), the SEMT in the geometry of a single brane is obtained as

$$\langle \tau_i^k \rangle_j^{(0)} = \delta_i^k \frac{4\xi - 1}{\alpha^D} \mathrm{PP}[F(s,z)]_{s=1}, \qquad (A2)$$

where $\mathrm{PP}[F(s,z)]_{s=1}$ corresponds to the finite part of the Laurent expansion of the function $F(s,z)$ near $s = 1$. The evaluation of that part is reduced to the extraction of the pole term.

The integral over $\mathbf{k}$ in Equation (A1) is expressed in terms of the gamma function and one obtains

$$F(s,z) = \frac{\mu^{s-1}\beta_j z^{D+1}}{2^{D-1}\pi^{D/2}} \frac{\Gamma(1 - \frac{D-s}{2})}{\Gamma(\frac{s}{2})} \int_0^\infty d\gamma\, \gamma J_\nu^2(\gamma z) \int_0^\infty d\lambda\, \lambda^2 \frac{(\lambda^2 + \gamma^2)^{\frac{D-s}{2}-1}}{1 + \lambda^2 \beta_j^2}. \qquad (A3)$$

For the further transformation of the expression on the right-hand side of Equation (A3) the integral representation

$$\left(\lambda^2 + \gamma^2\right)^{\frac{D-s}{2}-1} = \frac{1}{\Gamma\left(1 - \frac{D-s}{2}\right)} \int_0^\infty dx\, x^{\frac{s-D}{2}} e^{-(\lambda^2 + \gamma^2)x} \qquad (A4)$$

is used.

With this representation, the integral over γ is evaluated by the formula [61]

$$\int_0^\infty d\gamma\, \gamma J_\nu^2(\gamma z) e^{-\gamma^2 x} = \frac{1}{2x} \exp\left(-\frac{z^2}{2x}\right) I_\nu\left(\frac{z^2}{2x}\right), \qquad (A5)$$

with $I_\nu(u)$ being the modified Bessel function. Passing to a new integration variable $u = z^2/(2x)$, one finds

$$F(s,z) = \frac{\mu^{s-1}\beta_j z^{s+1}}{2^{\frac{D+s}{2}}\pi^{D/2}\Gamma(\frac{s}{2})} \int_0^\infty du\, u^{\frac{D-s}{2}-1} e^{-u} I_\nu(u) \int_0^\infty d\lambda\, \frac{\lambda^2 e^{-\lambda^2 \frac{z^2}{2y}}}{1 + \lambda^2 \beta_j^2}. \qquad (A6)$$

The λ-integral is evaluated in terms of the complementary incomplete gamma function $\Gamma(-1/2, x)$. As a result, the function $F(s,z)$ is presented as

$$F(s,z) = \frac{(\mu z)^{s-1}\beta_j z^2}{2^{\frac{D+s}{2}+2}\pi^{\frac{D-1}{2}}\Gamma(\frac{s}{2})|\beta_j|^3} \int_0^\infty du\, u^{\frac{D-s}{2}-1} S\left(2\beta_j^2/z^2, u\right), \qquad (A7)$$

where the function

$$S(b,u) = e^{-u} I_\nu(u) e^{\frac{1}{bu}} \Gamma\left(-\frac{1}{2}, \frac{1}{bu}\right) \qquad (A8)$$

is used.

In the limit $u \to \infty$, the function (A8) tends to the limiting value $\sqrt{2b/\pi}$ and $\lim_{u\to 0} S(b, u) = 0$. This shows that the representation (A7) is valid in the region $\operatorname{Re} s > D$ of the complex plane s.

The divergence of the integral in Equation (A8) at $s = 1$ comes from the divergence in the upper limit of the integral. By using the expansions of the functions $e^{-u} I_\nu(u)$ and $e^{\frac{1}{bu}}\Gamma\left(-\frac{1}{2}, \frac{1}{bu}\right)$ (see, e.g., [68]) for quite large values of u, the following expansion is obtained:

$$S(b, u) = \sqrt{\frac{2b}{\pi}} \sum_{n=0}^{\infty} \left[\frac{A_n(b)}{u^n} - \sqrt{\pi}\frac{B_n(b)}{u^{n+\frac{1}{2}}}\right]. \tag{A9}$$

For the coefficients, one has:

$$\begin{aligned}
A_0 &= 1, \ A_1 = \frac{2}{b} - \frac{1}{2}\left(\nu^2 - \frac{1}{4}\right), \\
A_2 &= \frac{4}{3b^2} + \left(\nu^2 - \frac{1}{4}\right)\left[\frac{1}{8}\left(\nu^2 - \frac{9}{4}\right) - \frac{1}{b}\right],
\end{aligned} \tag{A10}$$

and

$$\begin{aligned}
B_0 &= \frac{1}{\sqrt{b}}, \ B_1 = \frac{1}{b^{\frac{3}{2}}} - \frac{1}{2\sqrt{b}}\left(\nu^2 - \frac{1}{4}\right), \\
B_2 &= \frac{1}{2\sqrt{b}}\left[\frac{1}{b^2} + \left(\nu^2 - \frac{1}{4}\right)\left(\frac{1}{4}\left(\nu^2 - \frac{9}{4}\right) - \frac{1}{b}\right)\right].
\end{aligned} \tag{A11}$$

In order to separate the pole term in Equation (A7), let us rewrite the function $F(s, z)$ in the form

$$\begin{aligned}
F(s, z) &= \frac{(\mu z)^{s-1}\beta_j z^2}{2^{\frac{D+s}{2}+2}\pi^{\frac{D-1}{2}}\Gamma(\frac{s}{2})|\beta_j|^3}\Bigg\{\int_0^1 du\, u^{\frac{D-s}{2}-1}S(b_j, u) \\
&\quad + \int_1^\infty du\, u^{\frac{D-s}{2}-1}\left[S(b_j, u) - S_N(b_j, u)\right] + \int_1^\infty du\, u^{\frac{D-s}{2}-1}S_N(b_j, u)\Bigg\},
\end{aligned} \tag{A12}$$

where $b_j = 2\beta_j^2/z^2$ and

$$S_N(b, u) = \sqrt{\frac{2b}{\pi}} \sum_{n=0}^{N} \left[\frac{A_n(b)}{u^n} - \sqrt{\pi}\frac{B_n(b)}{u^{n+\frac{1}{2}}}\right]. \tag{A13}$$

For $N > (D - 3)/2$, the first two integrals in the curly brackets in Equation (A12) are convergent for $s = 1$. By using Equation (A13) in the last integral in Equation (A12), the corresponding contribution to the function $F(s, z)$ is presented as

$$\bar{F}(s, z) = -\frac{\left(\mu z/\sqrt{2}\right)^{s-1} z}{2^{\frac{D+1}{2}}\pi^{\frac{D}{2}}\Gamma(\frac{s}{2})\beta_j} \sum_{n=0}^{N}\left[\frac{A_n(b_j)}{s + 2n - D} - \frac{\sqrt{\pi}B_n(b_j)}{s + 1 + 2n - D}\right]. \tag{A14}$$

The function $\bar{F}(s, z)$ has a simple pole at $s = 1$. The pole comes from the term with $n = (D - 1)/2$ for odd D and from the term with $n = D/2 - 1$ for even D.

Expanding the function (A14) near the physical point $s = 1$, the function $F(s, z)$ is decomposed as

$$F(s, z) = \frac{F_{(\mathrm{p})}(s, z)}{s - 1} + F_{(\mathrm{f})}(z) + \cdots, \tag{A15}$$

where the unshown terms represent the part vanishing in the limit $s \to 1$. Here, the coefficient in the pole term reads

$$F_{(\mathrm{p})}(s, z) = -\frac{z C_D(b_j)}{(2\pi)^{\frac{D+1}{2}} \beta_j},$$

(A16)

and the finite term reads

$$
\begin{aligned}
F_{(\mathrm{f})}(z) &= \frac{\beta_j z^2}{2^{\frac{D+1}{2}+2} \pi^{\frac{D}{2}} |\beta_j|^3} \left\{ \int_0^1 du\, u^{\frac{D-3}{2}} S(b_j, u) + \int_1^\infty du\, u^{\frac{D-3}{2}} \left[S(b_j, u) - S_N(b_j, u) \right] \right\} \\
&+ \frac{z}{(2\pi)^{\frac{D+1}{2}} \beta_j} \left\{ C_D(b_j) \left[\ln\left(\frac{\mu z}{\sqrt{2}} \right) + \frac{1}{2} \psi(1/2) \right] - \sum_{n=0}^{N\prime} \left[\frac{A_n(b_j)}{1+2n-D} - \frac{\sqrt{\pi} B_n(b_j)}{2+2n-D} \right] \right\},
\end{aligned}
$$

(A17)

where the prime in the sum indicates that the term $n = (D-1)/2$ for odd D and the term $n = D/2 - 1$ for even D to be omitted. In Equation (A17), $\psi(x)$ is the digamma function with $\psi(1/2) \approx -1.964$ and

$$
C_D(b) = \begin{cases} A_{\frac{D-1}{2}}(b) & \text{for odd } D, \\ -\sqrt{\pi} B_{\frac{D}{2}-1}(b) & \text{for even } D. \end{cases}
$$

(A18)

In the principal part prescription, the physical value extracted from the divergent expectation value of the SEMT $\langle \tau_i^k \rangle_j^{(0)}$ is identified with

$$\langle \tau_i^k \rangle_j^{(0)} = \delta_i^k \frac{4\xi - 1}{\alpha^D} F_{(\mathrm{f})}(z).$$

(A19)

Note that this result contains a scale ambiguity. Under scale change it transforms to

$$\langle \tau_i^k \rangle_j^{(0)}(\mu') = \langle \tau_i^k \rangle_j^{(0)}(\mu) + \delta_i^k (4\xi - 1) \frac{\ln(\mu'/\mu) C_D(b_j) z}{(2\pi)^{\frac{D+1}{2}} \alpha^D \beta_j}.$$

(A20)

The logarithmic dependence on the scale μ is a distinctive feature of the regularization procedure.

References

1. Mostepanenko, V.M.; Trunov, N.N. *The Casimir Effect and Its Applications*; Clarendon Press/Oxford University Press: Oxford, UK, 1997. [CrossRef]
2. Milton, K.A. *The Casimir Effect: Physical Manifestation of Zero-Point Energy*; World Scientific: Singapore, 2002. [CrossRef]
3. Parsegian, V.A. *Van der Vaals Forces: A Handbook for Biologists, Chemists, Engineers, and Physicists*; Cambridge University Press: Cambridge, UK, 2005. [CrossRef]
4. Bordag, M.; Klimchitskaya, G.L.; Mohideen, U.; Mostepanenko, V.M. *Advances in the Casimir Effect*; Oxford University Press: Oxford, UK, 2009. [CrossRef]
5. Klimchitskaya, G.L.; Mohideen, U.; Mostepanenko, V.M. The Casimir force between real materials: Experiment and theory. *Rev. Mod. Phys.* **2009**, *81*, 1827–1885. [CrossRef]
6. Dalvit, D.; Milonni, P.; Roberts, D.; da Rosa, F. (Eds.) *Casimir Physics*; Springer: Berlin/Heidelberg, Germany, 2011. [CrossRef]
7. Avis, S.J.; Isham, C.J.; Storey, D. Quantum field theory in anti-de Sitter space-time. *Phys. Rev. D* **1978**, *18*, 3565–3576. [CrossRef]
8. Breitenlohner, P.; Freedman, D.Z. Stability in gauged extended supergravity. *Ann. Phys.* **1982**, *144*, 249–281. [CrossRef]
9. Mezincescu, L.; Townsend, P.K. Stability at a local maximum in higher dimensional anti-deSitter space and applications to supergravity. *Ann. Phys.* **1985**, *160*, 406–419. [CrossRef]
10. Saharian, A.A. Wightman function and Casimir densities on AdS bulk with application to the Randall-Sundrum braneworld. *Nucl. Phys. B* **2005**, *712*, 196–228. [CrossRef]
11. Ishibashi, A.; Wald, R.M. Dynamics in non-globally-hyperbolic static spacetimes: III. Anti-de Sitter spacetime. *Class. Quantum Grav.* **2004**, *21*, 2981–3014. [CrossRef]

12. Morley, T.; Taylor, P.; Winstanley, E. Quantum field theory on global anti-de Sitter space-time with Robin boundary conditions. *Class. Quantum Grav.* **2022**, *38*, 035009. [CrossRef]

13. Aharony, O.; Gubser, S.S.; Maldacena, J.; Ooguri, H.; Oz, Y. Large N field theories, string theory and gravity. *Phys. Rep.* **2000**, *323*, 183–386. [CrossRef]

14. Papantonopoulos, E. (Ed.) *From Gravity to Thermal Gauge Theories: The Ads/CFT Correspondence*; Springer: Berlin/Heidelberg, Germany, 2011. [CrossRef]

15. Năstase, H. *Introduction to AdS/CFT Correspondence*; Cambridge University Press: Cambridge, UK, 2015. [CrossRef]

16. Ammon, M.; Erdmenger, J. *Gauge/Gravity Duality: Foundations and Applications*; Cambridge University Press: Cambridge, UK, 2015. [CrossRef]

17. Pires, A.S.T. *AdS/CFT Correspondence in Condensed Matter*; Morgan & Claypool Publishers: San Rafael, CA, USA, 2014. [CrossRef]

18. Zaanen, J.; Sun, Y.-W.; Liu, Y.; Schalm, K. *Holographic Duality in Condensed Matter Physics*; Cambridge University Press: Cambridge, UK, 2015. [CrossRef]

19. Maartens, R.; Koyama, K. Brane-world gravity. *Living Rev. Relativ.* **2010**, *13*, 5. [CrossRef]

20. Fabinger, M.; Horava, P. Casimir effect between world-branes in heterotic M-theory. *Nucl. Phys. B* **2000**, *580*, 243–263. [CrossRef]

21. Nojiri, S.; Odintsov, S. Brane world inflation induced by quantum effects. *Phys. Lett. B* **2000**, *484*, 119–123. [CrossRef]

22. Nojiri, S.; Odintsov, S.; Zerbini, S. Quantum (in)stability of dilatonic AdS backgrounds and the holographic renormalization group with gravity. *Phys. Rev. D* **2000**, *62*, 064006. [CrossRef]

23. Toms, D.J. Quantised bulk fields in the Randall-Sundrum compactification model. *Phys. Lett. B* **2000**, *484*, 149–153. [CrossRef]

24. Nojiri, S.; Obregon, O.; Odintsov, S. (Non)-singular brane-world cosmology induced by quantum effects in five-dimensional dilatonic gravity. *Phys. Rev. D* **2000**, *62*, 104003. [CrossRef]

25. Goldberger, W.D.; Rothstein, I.Z. Quantum stabilization of compactified AdS_5. *Phys. Lett. B* **2000**, *491*, 339–344. [CrossRef]

26. Garriga, J.; Pujolàs, O.; Tanaka, T. Radion effective potential in the brane-world. *Nucl. Phys. B* **2001**, *605*, 192–214. [CrossRef]

27. Flachi, A.; Toms, D.J. Quantized bulk scalar fields in the Randall-Sundrum brane model. *Nucl. Phys. B* **2001**, *610*, 144–168. [CrossRef]

28. Flachi, A.; Moss, I.G.; Toms, D.J. Fermion vacuum energies in brane world models. *Phys. Lett. B* **2001**, *518*, 153–156. [CrossRef]

29. Brevik, I.H.; Milton, K.A.; Nojiri, S.; Odintsov, S.D. Quantum (in)stability of a brane-world AdS_5 universe at nonzero temperature. *Nucl. Phys. B* **2001**, *599*, 305–318. [CrossRef]

30. Flachi, A.; Moss, I.G.; Toms, D.J. Quantized bulk fermions in the Randall-Sundrum brane model. *Phys. Rev. D* **2001**, *64*, 105029. [CrossRef]

31. Naylor, W.; Sasaki, M. Casimir energy for de Sitter branes in bulk AdS_5. *Phys. Lett. B* **2002**, *542*, 289–294. [CrossRef]

32. Saharian, A.A.; Setare, M.R. The Casimir effect on background of conformally flat brane-world geometries. *Phys. Lett. B* **2003**, *552*, 119–126. [CrossRef]

33. Garriga, J.; Pomarol, A. A stable hierarchy from Casimir forces and the holographic interpretation. *Phys. Lett. B* **2003**, *560*, 91–97. [CrossRef]

34. Elizalde, E.; Nojiri, S.; Odintsov, S.D.; Ogushi, S. Casimir effect in de Sitter and anti-de Sitter braneworlds. *Phys. Rev. D* **2003**, *67*, 063515. [CrossRef]

35. Moss, I.G.; Naylor, W.; Santiago-Germán, W.; Sasaki, M. Bulk quantum effects for de Sitter branes in AdS_5. *Phys. Rev. D* **2003**, *67*, 125010. [CrossRef]

36. Saharian, A.A. Quantum vacuum effects in braneworlds on AdS bulk. *Universe* **2020**, *6*, 181. [CrossRef]

37. Knapman, A.; Toms, D.J. Stress-energy tensor for a quantized bulk scalar field in the Randall-Sundrum brane model. *Phys. Rev. D* **2004**, *69*, 044023. [CrossRef]

38. Saharian, A.A.; Mkhitaryan, A.L. Wightman function and vacuum densities for a Z_2-symmetric thick brane in AdS spacetime. *J. High Energy Phys.* **2007**, *08*, 063. [CrossRef]

39. Saharian, A.A. Wightman function and vacuum fluctuations in higher dimensional brane models. *Phys. Rev. D* **2006**, *73*, 044012. [CrossRef]

40. Saharian, A.A. Bulk Casimir densities and vacuum interaction forces in higher dimensional brane models. *Phys. Rev. D* **2006**, *73*, 064019. [CrossRef]

41. Shao, S.-H.; Chen, P.; Gu, J.-A. Stress-energy tensor induced by a bulk Dirac spinor in the Randall-Sundrum model. *Phys. Rev. D* **2010**, *81*, 084036. [CrossRef]

42. Elizalde, E.; Odintsov, S.D.; Saharian, A.A. Fermionic Casimir densities in anti-de Sitter spacetime. *Phys. Rev. D* **2013**, *87*, 084003. [CrossRef]

43. Kotanjyan, A.S.; Saharian, A.A. Electromagnetic quantum effects in anti-de Sitter spacetime. *Phys. At. Nucl.* **2017**, *80*, 562–571. [CrossRef]

44. Kotanjyan, A.S.; Saharian, A.A.; Saharyan, A.A. Electromagnetic Casimir Effect in AdS Spacetime. *Galaxies* **2017**, *5*, 102. [CrossRef]

45. Saharian, A.A.; Kotanjyan, A.S.; Sargsyan, H.G. Electromagnetic field correlators and the Casimir effect for planar boundaries in AdS spacetime with application in braneworlds. *Phys. Rev. D* **2020**, *102*, 105014. [CrossRef]

46. Randall, L.; Sundrum, R. Large mass hierarchy from a small extra dimension. *Phys. Rev. Lett.* **1999**, *83*, 3370–3373. [CrossRef]

47. Randall, L.; Sundrum, R. An alternative to compactification. *Phys. Rev. Lett.* **1999**, *83*, 4690–4693. [CrossRef]

48. Cuomo, G.; Mezei, M.; Raviv-Moshe, A. Boundary conformal field theory at large charge. *J. High Energy Phys.* **2021**, *10*, 143. [CrossRef]
49. Takayanagi, T. Holographic dual of a boundary conformal field theory. *Phys. Rev. Lett.* **2011**, *107*, 101602. [CrossRef]
50. Fujita, M.; Takayanagi, T.; Tonni, E. Aspects of AdS/BCFT. *J. High Energy Phys.* **2011**, *11*, 043. [CrossRef]
51. Ryu, S.; Takayanagi, T. Holographic derivation of entanglement entropy from the anti-de Sitter space/conformal field theory correspondence. *Phys. Rev. Lett.* **2006**, *96*, 181602. [CrossRef] [PubMed]
52. Ryu, S.; Takayanagi, T. Aspects of holographic entanglement entropy. *J. High Energy Phys.* **2006**, *08*, 045. [CrossRef]
53. Nishioka, T.; Ryu, S.; Takayanagi, T. Holographic entanglement entropy: An overview. *J. Phys. A Math. Theor.* **2009**, *42*, 504008. [CrossRef]
54. Chen, B.; Czech, B.; Wang, Z.-Z. Quantum information in holographic duality. *Rep. Prog. Phys.* **2022**, *85*, 046001. [CrossRef] [PubMed]
55. Bezerra de Mello, E.R.; Saharian, A.A.; Setare, M.R. Vacuum densities for a brane intersecting the AdS boundary. *Phys. Rev. D* **2015**, *92*, 104005. [CrossRef]
56. Bellucci, S.; Saharian, A.A.; Kotanjyan, V.K. Vacuum densities and the Casimir forces for branes orthogonal to the AdS boundary. *Phys. Rev. D* **2022**, *106*, 065021. [CrossRef]
57. Saharian, A.A. Energy-momentum tensor for a scalar field on manifolds with boundaries. *Phys. Rev. D* **2004**, *69*, 085005. [CrossRef]
58. Saharian, A.A. Surface Casimir densities and induced cosmological constant on parallel branes in AdS spacetime. *Phys. Rev. D* **2004**, *70*, 064026. [CrossRef]
59. Saharian, A.A. Surface Casimir densities and induced cosmological constant in higher dimensional braneworlds. *Phys. Rev. D* **2006**, *74*, 124009. [CrossRef]
60. Romeo, A.; Saharian, A.A. Casimir effect for scalar fields under Robin boundary conditions on plates. *J. Phys A Math. Gen.* **2002**, *35*, 1297–1320. [CrossRef]
61. Prudnikov, A.P.; Brychkov, Y.A.; Marichev, O.I. *Integrals and Series. Volume 2: Special Functions*; Gordon and Breach Science Publishers: Amsterdam, The Netherlands, 1998. Available online: https://archive.org/details/integralsseries0002prud (accessed on 20 November 2023).
62. Lebedev, S.L. Casimir effect in the presence of an elastic boundary. *J. Exp. Theor. Phys.* **1996**, *83*, 423–434. Available online: http://jetp.ras.ru/cgi-bin/e/index/e/83/3/p423?a=list (accessed on 20 November 2023).
63. Lebedev, S.L. Vacuum energy and Casimir force in the presence of a dimensional parameter in the boundary condition. *Phys. At. Nucl.* **2001**, *64*, 1337–1346. [CrossRef]
64. Elizalde, E.; Odintsov, S.D.; Romeo, A.; Bytsenko, A.A.; Zerbini, S. *Zeta Regularization Techniques with Applications*; World Scientific: Singapore, 1994. [CrossRef]
65. Kirsten, K. *Spectral Functions in Mathematics and Physics*; Chapman and Hall/CRC Press: Boca Raton, FL, USA, 2002. Available online: http://lib.ysu.am/disciplines_bk/70c8c6cffec7f1534b131c208088b6f4.pdf (accessed on 20 November 2023).
66. Elizalde, E. *Ten Physical Applications of Spectral Zeta Functions*; Springer: Heidelberg/Berlin, Germany, 2012. [CrossRef]
67. Blau, S.K.; Visser, M.; Wipf, A. Zeta functions and the Casimir energy. *Nucl. Phys. B* **1988**, *310*, 163–180. [CrossRef]
68. Abramowitz, M.; Stegun, I.A. (Eds.) *Handbook of Mathematical Functions: With Formulas, Graphs, and Mathematical Tables*; US Department of Commerce, National Bureau of Standarts: Washington, DC, USA, 1972. Available online: https://personal.math.ubc.ca/~cbm/aands/abramowitz_and_stegun.pdf (accessed on 20 November 2023).